Anat Embryol (1996) 194:13–22

ORIGINAL ARTICLE

Radma Mahmood · Ivor J. Mason
Gillian M. Morriss-Kay

Expression of *Fgf-3* in relation to hindbrain segmentation, otic pit position and pharyngeal arch morphology in normal and retinoic acid-exposed mouse embryos

Accepted: 12 December 1995

Abstract The gene *Fgf-3* is expressed in rhombomeres 5 and 6 of the hindbrain and has been functionally implicated in otic development. We describe new sites of expression of this gene in mouse embryos in the forebrain, the midbrain-hindbrain junction region, rhombomere boundaries, a cranial surface ectodermal domain that includes the otic placode, and in the most recently formed somite. In the early hindbrain, high levels of *Fgf-3* transcripts are present in rhombomere 4. The surface ectodermal domain at first (day 8½) extends laterally from rhombomeres 4 and 5 (prorhombomere B), in which neuroepithelial levels of expression are highest, to the second pharyngeal arch ventrally; at day 9, when the region of highest level of neuroepithelial *Fgf-3* expression is in rhombomeres 5 and 6, the dorsal origin of the surface ectodermal domain is also at this level, extending obliquely to the otic placode and the second arch. The initially high level of *Fgf-3* transcripts in the otic placode is downregulated as the placode invaginates to form the otic pit. *Fgf-3* is a good marker for the epithelium of pharyngeal arches 2 and 3, and our in situ hybridization results confirm the dual identity of the apparently fused first and second arches in some retinoic acid-exposed embryos, and the fusion of the first arch with the maxillary region in others. Correlation between *Fgf-3* expression and morphological pattern in craniofacial tissues of normal and retinoic acid-exposed embryos indicates that prorhombomere B, the second arch and the otic ectoderm represent a cranial segment whose structural integrity is maintained when hindbrain morphology and pharyngeal arch morphology are altered. Comparison of normal *Fgf-3* expression domains with those of *Fgf-4* and with the phenotype of *Fgf-3*-deficient mutant embryos suggests that there is some functional redundancy between *Fgf-3* and *Fgf-4* in otic induction and second arch development.

Key words Fibroblast growth factor · Tretinoin · Rhombencephalon · Pharyngeal arches · Developmental biology

R. Mahmood · G.M. Morriss-Kay (✉)
Department of Human Anatomy, South Parks Road,
Oxford OX1 3QX, UK
Tel.: (0)1865-272165; Fax: (0)1865-272420
e-mail: morrissk@vax.ox.ac.uk

R. Mahmood · I.J. Mason
MRC Brain Development Programme,
Division of Anatomy and Cell Biology,
UMDS Guy's and St Thomas' Hospitals,
London SE1 9RT, UK

Introduction

The mouse *Fgf-3* gene was formerly called *int-2*, having been originally identified as a common integration site for mouse mammary tumour virus, i.e. as a proto-oncogene (Dickson et al. 1984). It was subsequently recognised as a member of the fibroblast growth factor (FGF) family (Dickson and Peters 1987), and was renamed *Fgf-3* (Baird and Klagsbrun 1991). Its clearly defined domain of expression in rhombomeres (r) 5 and 6 of the embryonic hindbrain, adjacent to the position of the developing otocyst, led to the suggestion that it plays a key role in induction of the otocyst (Wilkinson et al. 1988).

Otic placodes are visible at the 8–10-somite stage as columnar epithelial regions within the otherwise squamous epithelium of the surface ectoderm (Kaufman 1992). They are situated on either side of the hindbrain neural folds level with the caudal half of the second pharyngeal arch, which is just beginning to form (O'Rahilly 1963). They rapidly invaginate to form otic pits and then, by the 23-somite stage, closed otocysts. By the 12- to 14-somite stage, r5 and r6 are clearly defined morphologically, and the otic pit can be seen to be adjacent to r5 and the rostral part of r6.

There is some evidence that inductive signals emanating from the neuroepithelium of the hindbrain influence the formation and later development of the otocyst (Harrison 1935; Van de Water and Ruben 1976). Wilkinson et al. (1988, 1989) suggested that *Fgf-3* might be one such signal. This hypothesis was supported by the observation

that otocyst formation in chick embryos was blocked by antisense oligonucleotides to FGF-3 protein and by antibodies against FGF-3 in explant culture (Represa et al. 1991). However, mice homozygous for a targeted disruption of the *Fgf-3* gene form otocysts that are normal in morphology but whose subsequent morphogenesis and differentiation are aberrant (Mansour et al. 1993). Similarly, in the *kreisler* mutant mouse, in which *Fgf-3* is expressed at very low levels (Frohman et al. 1993; McKay et al. 1994), the otocyst forms but fails to undergo normal morphogenesis and differentiation (Deol 1964).

In order to obtain further information on the relationship between otocyst formation and *Fgf-3* expression, we have studied mouse embryos exposed to retinoic acid (RA). Embryos exposed to high levels of RA at the late presomite stage (day 7¾) develop craniofacial defects, one of the earliest morphological features of which is an abnormally rostrally-positioned otocyst (Morriss-Kay et al. 1991). The relationship between the developing otocyst and the rhombomeres is not clear in RA-treated embryos, since rhombomeric segmentation is suppressed, but its position is normal with respect to the expression patterns of *Krox-20* and *Hoxb-3* (Wood et al. 1994). Rat embryos exposed to retinoid excess at similar stages show identical malformations to those of mouse embryos, and (unlike mouse) survive to term, at which stage the inner ear is still abnormal in position but apparently normal in histological structure (Morriss 1972; Morriss and Thorogood 1978; G.M. Morriss, and P.V. Thorogood, unpublished material). These data indicate that normal morphogenesis and differentiation can occur in an ectopically-positioned otocyst in the absence of normal hindbrain morphology and gene expression. Since *Fgf-3* expression is morphologically and possibly functionally linked to otocyst development, the effects of RA treatment on the expression of this gene are clearly of interest. Indeed, upregulation of *Fgf-3* by RA has been demonstrated in embryonal carcinoma cells and F9 cells (Smith et al. 1988; Mansour and Martin 1988; Grinberg et al. 1991; Murakami et al. 1993).

We have here used in situ hybridization to localize *Fgf-3* transcripts in normal and RA-treated embryos in order to discover whether the rostral shift in otic pit and pharyngeal arch position is linked with a corresponding shift in hindbrain *Fgf-3* expression, and to investigate the relationship between *Fgf-3* expression and rhombomeric segmentation. We have also made a careful study to localise *Fgf-3* in previously unreported sites in normal embryos.

Materials and methods

Mouse matings and RA treatment

Pregnant female mice (C57Bl/6) weighing a mean of 25 g, received by oral gavage 12 mg/kg all-*trans*-RA in arachis oil (0.6 ml per mouse) at 7¾ and 8¼ days of development (for details see Morriss-Kay et al. 1991). At 8½ days of development (18 h after exposure to RA on day 7¾) and 9 or 9½ days of development (30 or 42 h after exposure on day 7¾ or 8¼), embryos were explanted into Tyrode's saline, examined for malformations, and fixed for 4 h in 4% paraformaldehyde at 4°C. Control embryos of equivalent ages were obtained from dams given 0.6 ml of vehicle only. After fixation, embryos were processed for in situ hybridization. Animal care and experimental procedures were carried out under U.K. Home Office licence.

Fgf-3 probes and in situ hybridization

^{35}S-labelled single-stranded sense and antisense probes were prepared by transcribing *Fgf-3* fragments from linearized SP65 and SP64 vectors respectively. Both probes were approximately 1.6kb in length and were composed of residues 5676–7368 of the *Fgf-3* gene (Moore et al. 1986). Radioactive in situ hybridization was performed as described by Wilkinson et al. (1987a, b) with minor modifications as outlined by Morriss-Kay et al. (1991). Exposure times ranged between 4 and 5 weeks; after developing, sections were stained with Ehrlich's haematoxylin, and examined by both brightfield and darkfield illumination. Non-radioactive in situ hybridzation was performed on whole embryos as described by Wilkinson (1992), with minor modifications as outlined by Mahmood et al. (1995a).

Results

Morphological appearance after exposure to retinoic acid: whole and sectioned embryos

The effects of retinoic acid on morphogenesis were dependent on the precise stage of exposure, as described previously (Wood et al. 1994). Briefly, embryos exposed to RA at the presomite stage (day 7¾) (Figs. 1C, 2B, 4G,L) showed no preotic sulcus at day 8½ and no hindbrain (rhombomeric) segmentation at day 9½; at day 9/9½ the preotic hindbrain was shorter than that of control embryos, with concomitant rostral shift of the otic pits and apparent fusion of the first pharyngeal arch with the maxillary region of the face. The otic pits were separated from the hindbrain neuroepithelium by mesenchyme (Fig. 4L); this mesenchymal tissue is thought to be neural crest-derived on the basis of its expression of *Krox-20* (Morriss-Kay et al. 1991). Embryos exposed to RA on day 8¼, i.e. after the onset of somitic segmentation, showed slight shortening of the preotic hindbrain and rhombomeric segmentation of variable form (Figs. 1B, 4H); the first pharyngeal arch appeared to be fused with the second.

Expression of *Fgf-3* in 8½-day embryos (Figs. 2, 3)

Control embryos examined on day 8½ ranged from the 4- to 10-somite stages. The distribution of RNA transcripts in hindbrain neuroepithelium extended from the midbrain/hindbrain junction to a level caudal to the preotic sulcus, the most intense signal being in the caudal part of this domain, i.e in prorhombomere B; by the 6-somite stage, the expression domain extended into the rostral part of prorhombomere C (Fig. 2A). At this stage, expression was also observed in the surface ectoderm immediately lateral to prorhombomere B, extending ven-

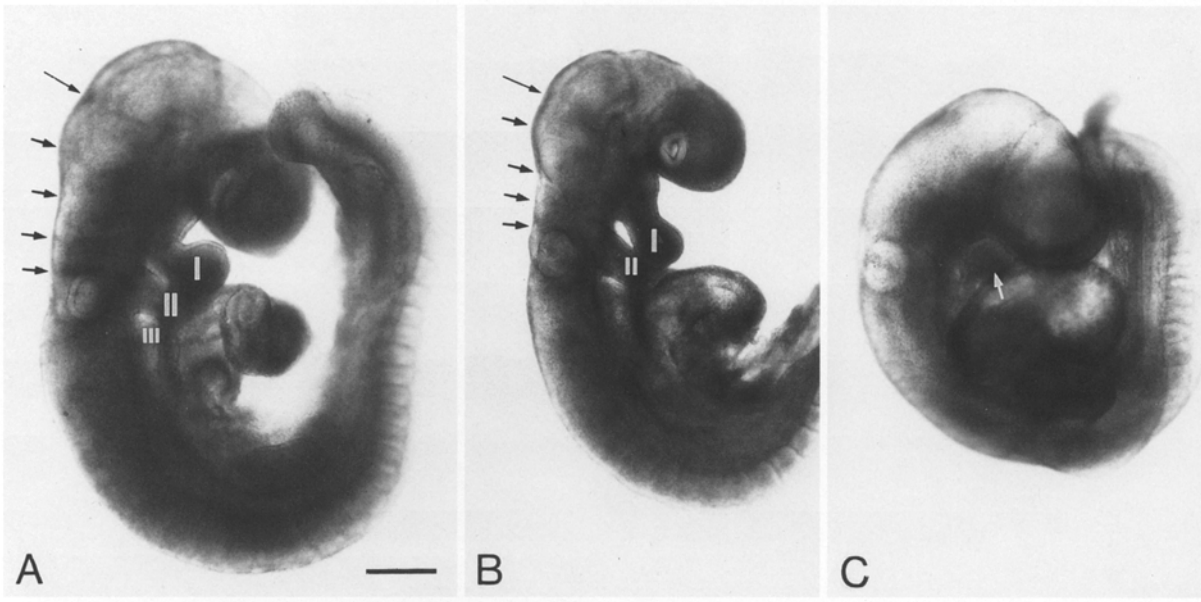

Fig. 1 Live embryos, day 9½, to show the morphology of the first and second pharyngeal arches and their positional relationship to the otocyst: **A** control, **B**,**C** retinoic acid (RA)-treated. **A** In a control embryo, the bulbous first arch (*I*) is separated by a gap from the maxillary region; the rostral border of the otocyst is level with the middle of the second pharyngeal arch (*II*) and the caudal border is level with the second pouch. A small third arch (*III*) is also present. The midbrain/hindbrain boundary and the rhombomeric boundaries 1/2, 2/3, 3/4 and 4/5 can be distinguished in the hindbrain (*arrows*). **B** In an embryo exposed to RA on day 8¼, the gap between the first arch and maxillary region is lost, but the otocyst position, relative to the arches, is normal. The preotic hindbrain is shorter than that of the control; rhombomeric segmentation is present, the boundaries being closer together than those of the control embryo (*arrows*). **C** In an embryo exposed to RA on day 7¾, a large pharyngeal arch (*white arrow*) situated level with the otocyst and beneath the maxillary region and the forebrain. It is not clear whether this represents the first arch, the second arch, or a fusion of the two. The midbrain/hindbrain boundary is unclear and the hindbrain is unsegmented. *Bar* 250 μm

trally to the area of the future second pharyngeal arch (Fig. 2C). *Fgf-3* was also expressed in the primary mesenchyme newly emergent from the primitive streak (Fig. 2A). Following exposure to RA on day 7¾, *Fgf-3* expression in the primary mesenchyme of 6-somite stage embryos was equivalent to that of controls (Fig. 2D c.f. 2A), but the hindbrain domain was more extensive (Fig. 2B). *Fgf-3* expression in dorsolateral surface ectoderm was equivalent in intensity to that observed in control embryos but more rostral in position (Fig. 2D).

At the 10-somite stage (Fig. 3), *Fgf-3* expression in control embryos was detected in both ectoderm and endoderm of the second arch, but the dorsolateral surface ectodermal domain was now oblique, linking the second arch domain to rhombomere (r)5 (Fig. 3A). This domain includes the otic placode, situated between the neuroepithelium of r5/6 dorsally and the caudal part of the second arch ventrally (Fig. 3B and adjacent sections; see also Kaufman 1992). In the neuroepithelium, the highest level of *Fgf-3* transcripts was, as previously described (Wilkinson et al. 1988), located in r5 and r6 of the hindbrain, but high levels of expression were also observed in r4 and in the r2/3 boundary (Fig 3B). RA-treated embryos were not examined at this somite stage.

Expression of *Fgf-3* in 9-day embryos (Fig. 4, A–D)

In control day 9 embryos (16- to 20-somite stages), *Fgf-3* expression was weak in r1–r4 except at the rhombomeric boundaries; transcripts were present in parts of the otic pit, particularly the caudal edge, in the caudal midbrain and in the ventral forebrain, and there was some weak expression throughout r1–r4 (Fig. 4A,B). The second arch expression domain was still linked to r5 by a surface ectodermal domain, but a new third arch domain was separate (Fig. 4A). There was a small domain of expression in the posterior part of the most recently formed somite (Fig. 4A). In RA-exposed embryos of equivalent somite stages, hindbrain neuroepithelial expression was upregulated compared with that of controls, and was divided into rostral and caudal domains (Fig. 4C,D). The surface ectodermal expression domain was broader than that of day 9 control embryos; it extended towards the second arch domain but was not continuous with it (Fig. 4C). Expression in the otic pit (Fig. 4D) was similar to that of control embryos.

Expression of *Fgf-3* in 9½-day embryos (Fig. 4, E–L)

In day 9½ control embryos, the weak expression within r1–4 was downregulated but expression in boundary cells was retained; expression in r5 was downregulated before that in r6 (Fig. 4E,F,J). Pharyngeal arch expression was confined to the rostral ectoderm and endoderm of arches 2 and 3 (Fig. 4E,F,I), and the otic surface ectodermal domain was downregulated (Fig. 4F).

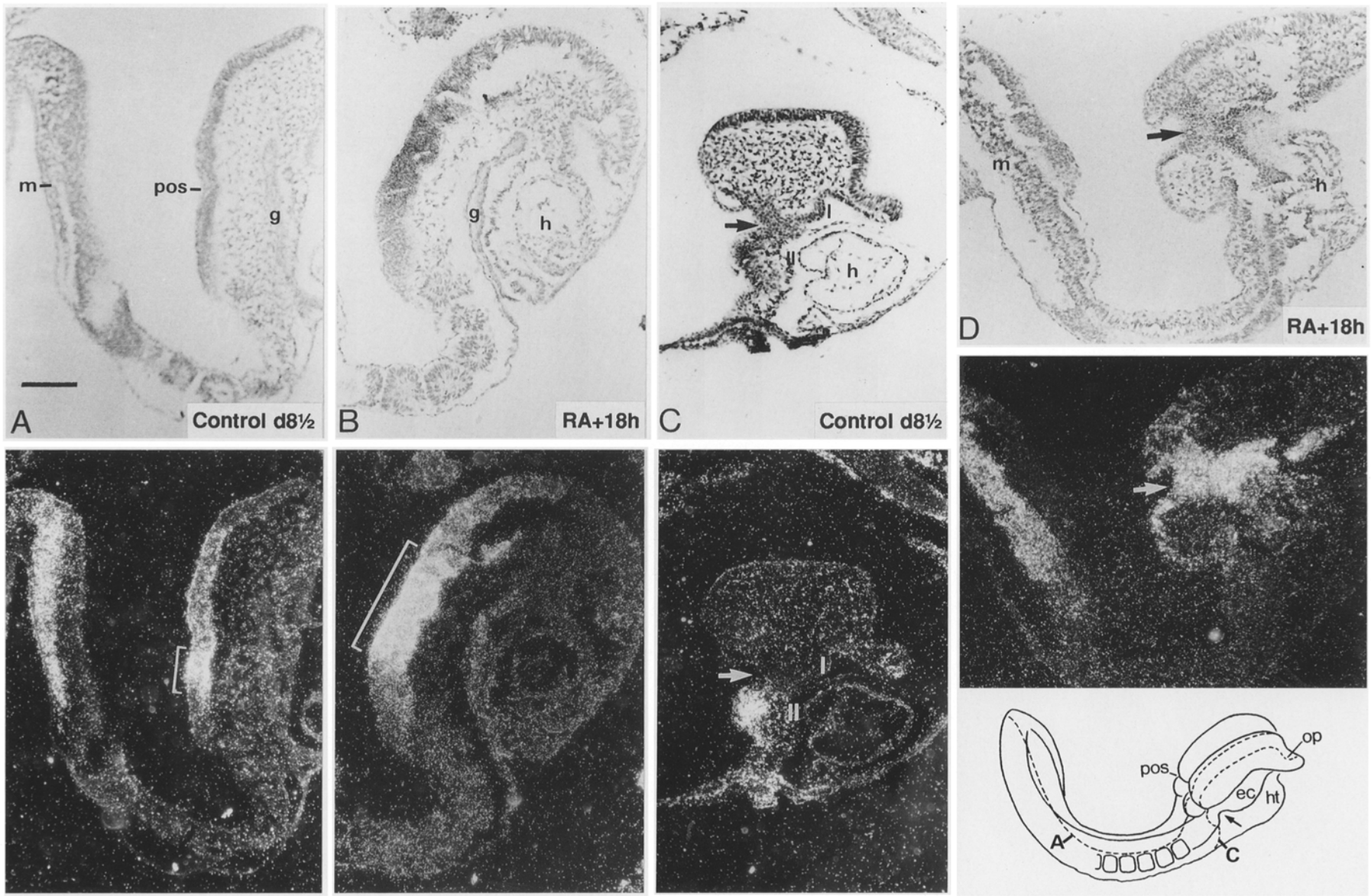
m
pos
g
A
Control d8½
g
h
B
RA+18h
I
II
h
C
Control d8½
m
h
D
RA+18h
I
II
op
pos
ec
ht
A
C

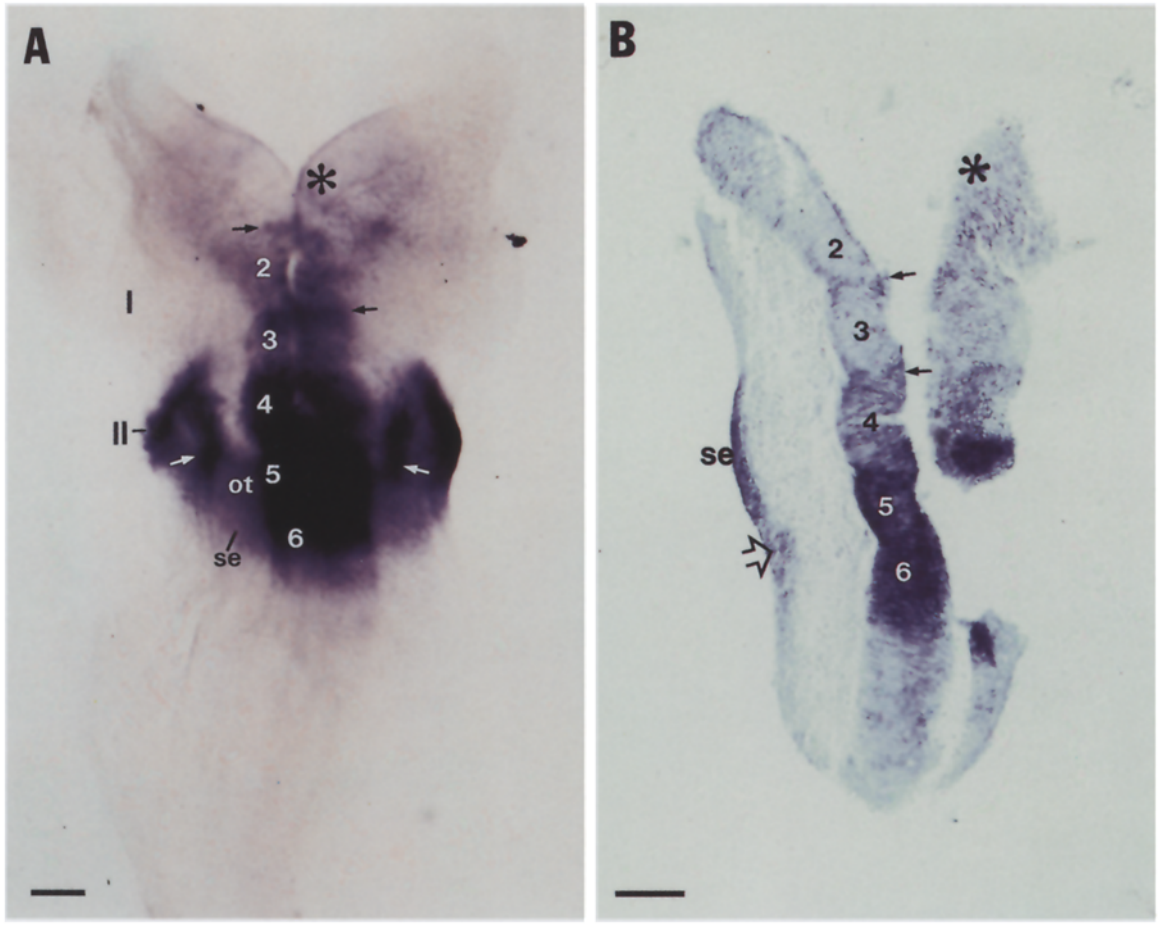

Fig. 3 **A** Whole 10-somite stage (late day 8) untreated embryo, dorsal view, hybridized with *Fgf-3* probe. High levels of *Fgf-3* transcripts are present in r4-6, in the r1/2 and 2/3 boundaries (*black arrows*), in the ectoderm (*II*) and endoderm (*white arrows*) of the second pharyngeal arch. Surface ectodermal expression (*se*) extending as an arc from the level of r5/6 to the second arch on each side includes the otic placode (*ot*) adjacent to the neuroepithelium. The *asterisk* indicates the position asterisked in **B**. **B** Coronal section of the same embryo, cut close to or just above the dorsal surface on the *right side*, and deep to the surface on the *left*. Surface ectodermal staining includes ectoderm dorsal to the second arch (*se*) and the ventral edge of the otic placode (*open arrow*). Gyrus cells at the r3/4 boundary show *Fgf-3* transcripts. Other features and labels as in **A**. *Bar* 100 μm

In embryos exposed to RA on day 8¼ (Fig. 4G,K), *Fgf-3* expression in the hindbrain was variable. In contrast to control embryos of the same age, the r5/6 domain showed a higher level of transcripts in r5 than in r6 (compare Fig. 4G with 4F, and Fig. 4 K with 4J); the "boundary domains" did not precisely coincide with morphological boundaries, some apparently segmental domains being within rhombomeric sulci (Fig. 4 K). Expression was upregulated in the midbrain/hindbrain junction region, and ectopic expression was observed in the midbrain (Fig. 4G). The second and third pharyngeal arch domains covered the full breadth of the arches, instead of being confined to the rostral aspects as in control embryos (compare Fig. 4G with 4F); dorsolateral surface ectodermal expression was downregulated, as in controls.

In embryos treated with RA on day 7¾, the *Fgf-3* expression domain in the caudal midbrain/rostral hindbrain was more extensive than normal (Fig. 4H,L). The level of transcripts in the forebrain was comparable with that of controls. There was an ectopic midbrain domain (*ar-*

Fig. 2 Parasagittal sections close to the midline (**A**, **B**) and more lateral (**C**, **D**) of day 8½ control and RA-exposed embryos as indicated; brightfield (*top row*) and darkfield (*bottom*) showing *Fgf-3* transcript domains. The diagram (*bottom right*) shows the point of entry of the knife in *A* and *C*. The sections shown in **B** and **D** are slightly oblique, so that the tail region is on **D**, together with the more lateral head section. **A** In control embryos, the *Fgf-3* domain extends from the caudal midbrain to prorhombomere B, in which the level of transcripts is highest (indicated by the *bracket*); a lower level of transcripts extends a short distance into prorhombomere C. **B** The preotic sulcus is absent from RA-exposed embryos; the *Fgf-3* domain is shifted rostrally and the area of highest transcript levels (*bracket*) is more extensive than in controls. **C** More lateral section of a control embryo showing *Fgf-3* transcripts in the surface ectoderm continuous with prorhombomere B, extending ventrally towards the nascent second arch (*II*). The *arrow* indicates the developing first pharyngeal cleft, which is immediately lateral to the preotic sulcus. **D** RA-exposed embryo showing rostral shift of the surface ectodermal domain (*arrow*). Expression of *Fgf-3* in mesoderm (*m*) close to the primitive streak is unaltered (compare with **A**). *ec* Surface ectoderm, *g* foregut, *ht* heart, *m* primary mesenchyme, *op* optic sulcus, *pos* preotic sulcus, *arrow* first pharyngeal cleft, *I*, *II* first and second pharyngeal arches. *Bar* 100 μm

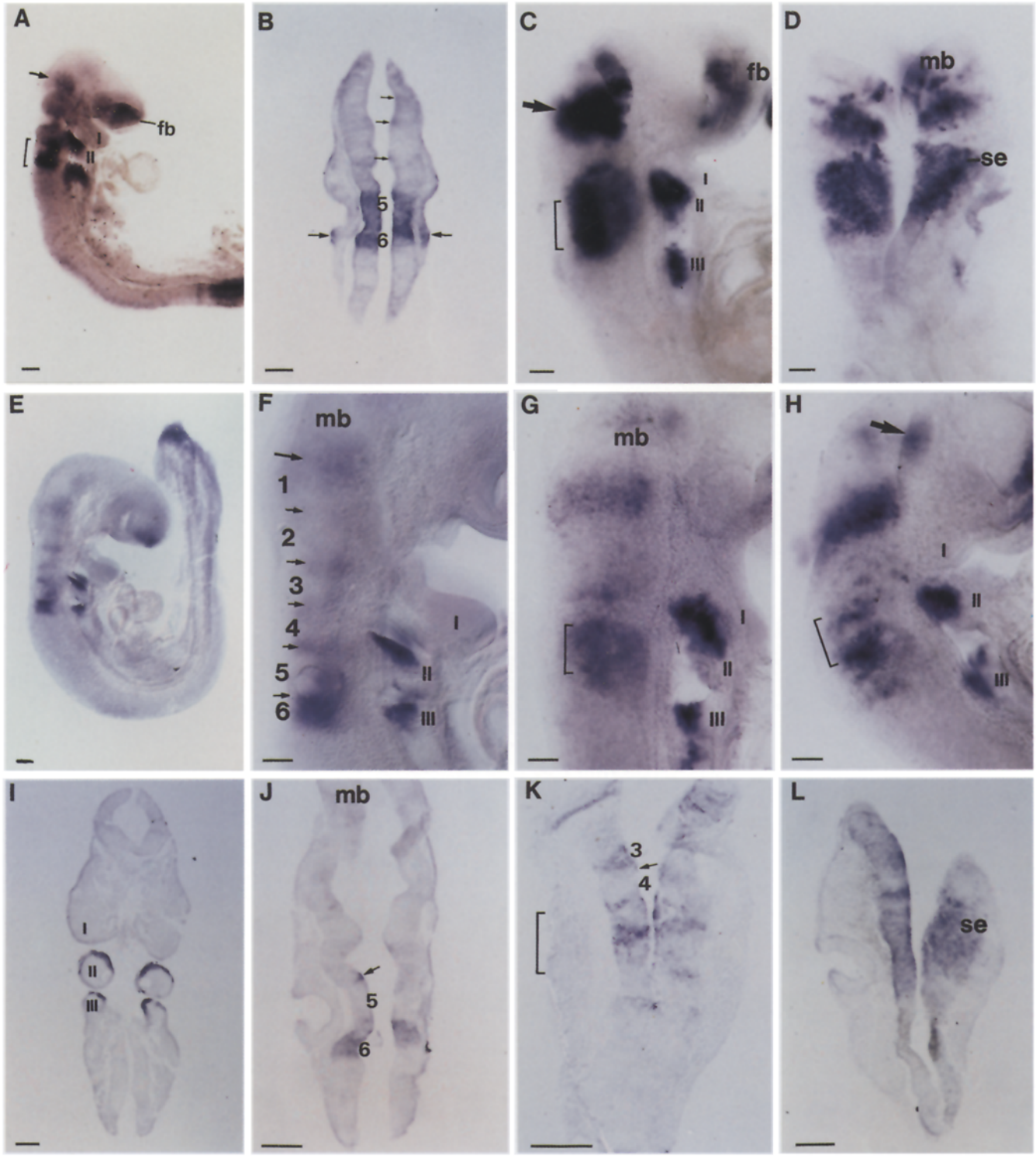

Fig. 4A–L Whole embryos and sections, day 9/9½, hybridized with *Fgf-3* probe. Where not obvious, the otic pit is indicated by a *square bracket*. **A** Day 9 (19-somite stage) control embryo showing *Fgf-3* transcripts in the neuroepithelium of the forebrain (*fb*), the midbrain/hindbrain junction region (*arrow*) and r1-6 (highest in r5/6, level with the otic pit), and in the second and third pharyngeal arches. Caudally, transcripts are present in the segmental plate and in the most recently formed somite. **B** Coronal section through the hindbrain of the embryo shown in **A**, showing high transcript levels in r1/2, r2/3 and r3/4 boundary cells, at the caudal edge of the otic epithelium (*arrows*), in the whole of r5 and most of r6. **C** Day 9 embryo exposed to RA on day 7¾: *Fgf-3* transcript domains are in the forebrain (*fb*), midbrain/hindbrain junction (*arrowed*), otic hindbrain, second arch (which is fused with the first) and third arch. **D** Dorsal view of the same embryo, focused on the surface ectodermal domain (*se*), which is continuous with the most caudal neuroepithelial domain. **E, F** Control embryo, day 9½ (26-somite stage), showing *Fgf-3* expression domains in the forebrain, the midbrain/hindbrain and rhombomeric junctions (*arrowed*), r6, and arches two and three. **G** Day 9½ embryo exposed to RA on day 8¼: fused first and second arches; ectopic midbrain *Fgf-3* domain. **H** Day 9½ embryo exposed to RA on day 7¾: first arch

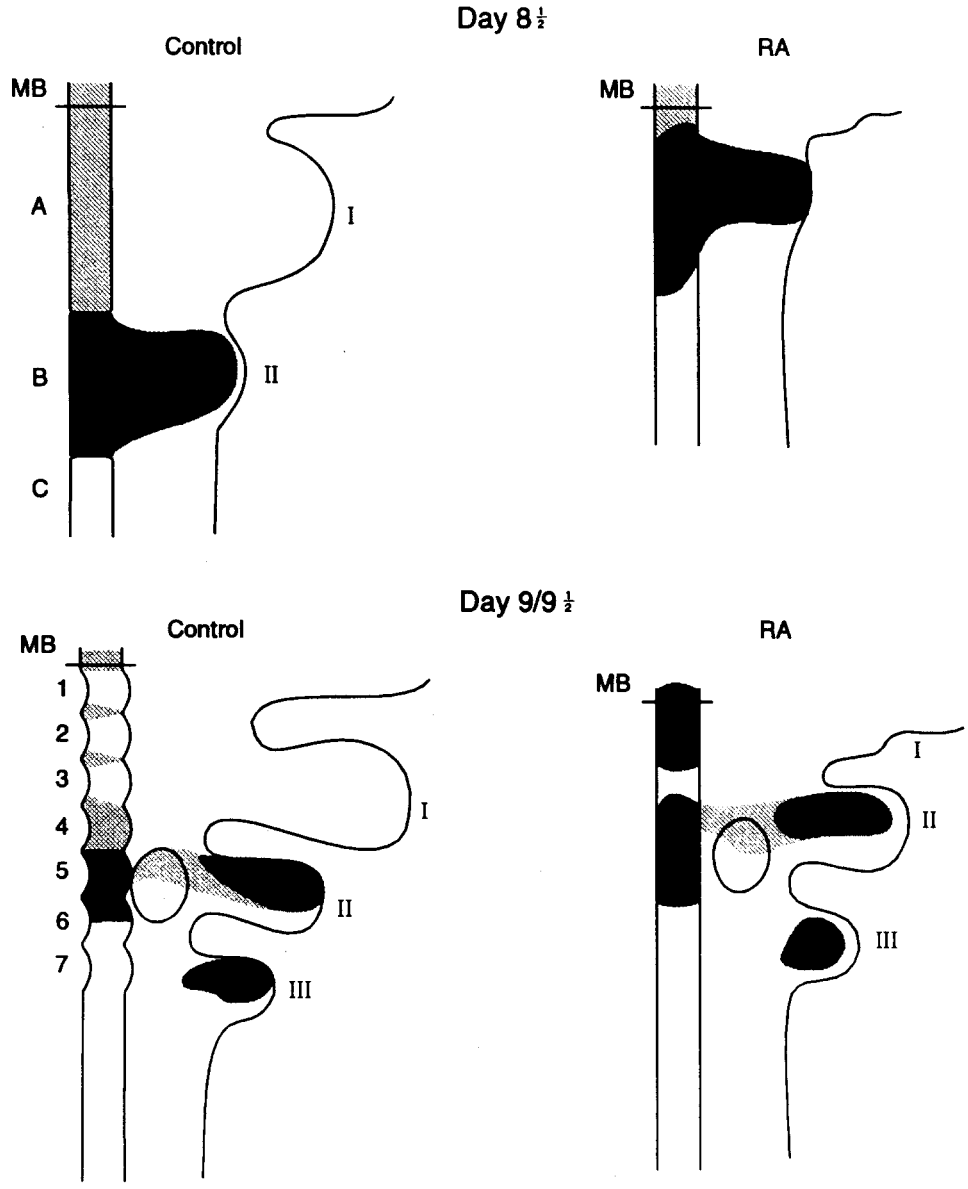

Fig. 5 Diagrammatic summary of the hindbrain, surface ectodermal and pharyngeal arch domains of *Fgf-3* expression in control embryos (*left*) and embryos exposed to RA on day 7¾ (*right*) as in Figs. 2–4 and equivalent specimens. The day-8½ control embryo is shown before extension of the domain of highest level of expression extends into prorhombomere C (future r6); the surface ectodermal domain at this stage extends laterally from prorhombomere B (future r4/5). The day 9/9½ expression patterns are composites; the surface ectodermal domain linking the neural tube (r5) and second arch was present at day 9 but downregulated by day 9½ in all control and most RA-exposed embryos. *MB* Midbrain

rowed in Fig. 4H). In the hindbrain, which was unsegmented, neuroepithelial expression of *Fgf-3* was patchy and irregular; in some embryos there was still some surface ectodermal expression continuous with the neuroepithelial domain, although expression had been downregulated in the otic pit (Fig. 4L).

fused with maxillary region; ectopic midbrain *Fgf-3* domain (*arrow*). **I** Control day 9½ embryo: coronal section showing second and third arch epithelial domains of *Fgf-3*. **J** More dorsal coronal section of the same embryo, showing downregulation of rhombomeric *Fgf-3* expression except in r6, the midbrain/hindbrain boundary region and some rhombomeric boundary cells (*arrow*; other boundaries are stained on adjacent sections). **K** Coronal section of a day 9½ embryo exposed to RA on day 8¼, showing periodic *Fgf-3* domains that do not correspond to morphological rhombomeric boundaries, e.g. expression in r3 (the r3/4 gyrus is *arrowed*). **L** Coronal section of a day 9½ embryo exposed to RA on day 7¾, showing patchy and irregular *Fgf-3* expression the unsegmented neuroepithelium (*left*) and maintenance of the surface ectodermal domain (*right*). *mb* Midbrain, *se* surface ectoderm, *I*, *II*, *III* pharyngeal arches one to three. *Bars* 100 μm

Positional relationships between the otic pit, the second pharyngeal arch, and hindbrain *Fgf-3* expression

In embryos exposed to RA at the early somite stage (day 8¼), the first pharyngeal arch was partially or completely fused with the second (Figs. 1B, 4G). In embryos exposed to RA at the late presomite stage (day 7¾), the first arch appeared to be fused with the maxillary process (Figs. 1C, 4H). The pattern of expression of *Fgf-3* correlated well with this morphological interpretation: where arches I and II were fused, *Fgf-3* expression was present only in the caudal half of the fused structure, apparently defining the second arch territory (Fig. 4G); where arch I was fused with the maxillary region, *Fgf-3* expression

was present the full width of the first definitive arch, indicating that this was actually arch II (Fig. 4H). A second patch of expression defined the third arch territory in both types of abnormal embryo (Fig. 4G,H).

In control day 9 and day 9½ embryos, the otic pit/otocyst was level with the caudal half of the second pharyngeal arch and with the second pharyngeal cleft. In embryos exposed to RA at both early somite and late presomite stages, otic pit position was normal with respect to the second pharyngeal arch-related domain of *Fgf-3* expression (Fig. 4F–H). Therefore, shortening of the preotic hindbrain, which resulted in rostral shift of the otic pit, had also resulted in an equivalent rostral shift of the pharyngeal arches and of hindbrain *Fgf-3* expression domains. The otic surface ectodermal domain of *Fgf-3* was also shifted rostrally, at a stage prior to the time of differentiation of the otic placode (compare Fig. 2C,D). These relationships suggest that the site of induction of the otic placode is fixed in relation to the hindbrain neuroectodermal domain, the surface ectodermal domain, and the second pharyngeal arch domain of *Fgf-3* expression.

Discussion

Previous studies on *Fgf-3* (*int-2*) expression domains in the mouse have reported expression in primary mesenchyme, in r5/6, and in the endoderm of pharyngeal pouches 1 to 3 (Wilkinson et al. 1988). In this study, we report new sites of *Fgf-3* expression in the mouse embryo: by using wholemount in situ hybridization methods, we have additionally identified *Fgf-3* expression in the ventral forebrain, at the midbrain/hindbrain junction, in rhombomeric boundary cells, in r4, in a domain of surface ectodermal expression extending from the level of r4/5 (later r5/6) to the second pharyngeal arch at early somite stages, in the rostral epithelium of pharyngeal arches 1 and 2, and in the most recently formed somite. The surface ectodermal domain of *Fgf-3* includes the otic placode, in which it is downregulated during otic pit invagination. In addition to these observations in normal embryos, we have examined the relationship between *Fgf-3* expression, otocyst position, hindbrain morphology and pharyngeal arch morphology in embryos exposed to RA at stages that alter the morphogenesis of these structures.

Functions of *Fgf-3*

Studies on *Fgf-3* null mutant embryos (Mansour et al. 1993) and the *Fgf-3*-deficient *kreisler* mutant (Deol 1964; Frohman et al. 1993; McKay et al. 1994) indicate that *Fgf-3* essential for late stages of otic morphogenesis and differentiation but not for induction of the otic placode or for otocyst formation; a function for *Fgf-3* in somite development is indicated by vertebral defects in the null mutant, but these defects are restricted to the tail. The functional requirement for *Fgf-3* is therefore limited to a minority of the expression domains reported here; this observation suggests that *Fgf-3* protein may play a greater role normal development than is revealed by the study of mutants, and that there may be functional redundancy with other Fgf proteins through a common receptor-mediated signalling pathway. Expression domains coincidental with those of *Fgf-3* include *Fgf-4* in both cranial surface ectodermal and pharyngeal arch epithelial domains (Niswander and Martin 1992) and *Fgf-8* in pharyngeal arch epithelia (Crossley and Martin 1995; Mahmood et al. 1995b). No other Fgf has been observed in newly formed somites, although *Fgf-1*, *-2*, *-4*, *-6*, *-7* and *-8* are expressed in later somitic myotome (Mason et al. 1994 and references therein; Crossley and Martin 1995; Mahmood et al. 1995b). *Fgf-4* and *Fgf-8* are both present in the unsegmented primary mesenchyme, and, together with *Fgf-3*, may play a role in trunk somitogenesis, but there are no reported observations of *Fgf* expression in relation to tail development that might elucidate the apparently unique role of *Fgf-3* in tail segmentation.

Fgf-3 in rhombomeric boundary cells and at the midbrain-hindbrain junction

Fgf-3 is unusual in being expressed both in developing somites and in rhombomeres. A similar (but better defined) pattern has been observed in the chick embryo (Mahmood et al. 1995a) but not in *Xenopus* (Tannahill et al. 1992). *Sek-1* (originally named *Sek*) is also expressed during both rhombomere formation and somitogenesis in mouse embryos (Nieto et al. 1992); *Sek-1* expression in rhombomeres shows a segmental pattern an earlier stage than that shown here for *Fgf-3*, so is more likely than *Fgf-3* to play a role in the segmentation process. In RA-exposed embryos, the degree of failure of boundary-related *Fgf-3* expression was correlated with the degree of suppression of segmentation: it was completely absent in the unsegmented hindbrain neuroepithelium of embryos exposed to RA on day 7¾, and present but not strictly related to rhombomeric gyri in embryos exposed to RA on day 8¼, in which segmentation is present but often irregular or poorly defined. These data from normal and RA-exposed embryos support the interpretation that maintenance of expression of *Fgf-3* in rhombomeric boundaries in normal development is unrelated to the formation of rhombomeres as morphological structures.

Fgf-3 expression was also observed at the midbrain/hindbrain junction, where it was upregulated following exposure to RA. This region, which gives rise to the cerebellum and pons, develops abnormally in human embryos exposed to RA in utero: cellular organisation and differentiation is abnormal, and the cerebellum is reduced in size (Lammer and Armstrong 1992). At later stages of cerebellar development, *Fgf-3* is expressed in Purkinje cells (Wilkinson et al. 1989). These observations suggest that *Fgf-3* may play a determinative role in

the events leading to cerebellar formation and differentiation.

Fgf-3 expression in the hindbrain and otic ectoderm

The developing pattern of *Fgf-3* expression within the hindbrain begins as a continuous domain throughout prorhombomeres A and B, subsequently extending to include the rostral part of prorhombomere C. The prorhombomere B/C (r4/5/6) domain shows the highest level of expression; from this level a surface ectodermal domain extends laterally into the epithelium of the nascent second pharyngeal arch, giving the appearance of a segmental band equivalent to the ectodermal cranial segments or "ectomeres" that have been demonstrated in avian embryos (Couly and Le Douarin 1990). The surface ectodermal component of this segmental domain includes the otic placode. In early somite-stage embryos that have been exposed to RA at presomite stages (day 7¾), this whole band of *Fgf-3* expression is shifted rostrally. By later somite stages (day 9 and 9½) it can be seen that the rostral shift includes the otic pit, the otic neuroepithelium (identified by its characteristic r5/6 pattern of *Fgf-3* expression), and the first and second pharyngeal arches.

Confirmation that the otic pit maintains its positional relationship with r5 comes from previous studies of embryos exposed to RA at presomite stages, in which the r5 domains of expression of *Krox-20* and *Hoxb-3* were normal with respect to the otic pit, although rhombomeric segmentation was absent and *Hoxb-1*, normally confined to r4, was expressed throughout the preotic hindbrain (Morriss-Kay et al. 1991; Wood et al. 1994). These studies on rhombomere-specific gene expression patterns, taken together with the results presented here, show that the normal positional relationships between *Fgf-3* domains in the r4/5/6 neuroepithelium, the second pharyngeal arch epithelium, and the otic surface ectoderm that links them, is clearly maintained in RA-exposed embryos. The otocyst in RA-exposed embryos should therefore not be regarded as ectopic, having maintained its relationship to other structures and to their pattern of expression of *Fgf-3*, *Hoxb-3* and *Krox-20*. Rather, the whole of the embryonic segment that includes prorhombomere B, the otic ectoderm and the second arch has shifted rostrally as a consequence of the RA-induced shortening and respecification of the preotic hindbrain. This embryonic segment therefore has a functional integrity that is not disrupted by RA-induced alterations in morphogenesis. Non-ectodermal components of this segment also show specific domains of gene expression: a discrete mesodermal domain of *Sek-2* underlies the ectodermal band of *Fgf-3* (Becker et al. 1994), and early and later emigrating populations of neural crest cells expressing *CRABP I* and *Hoxb-1* migrate respectively from prorhombomere B to the second arch (Ruberte et al. 1991), and from r4 to form the acousticofacial ganglion (Hunt et al. 1991).

Fgf-3 and otic induction in normal and RA-exposed embryos

In normal embryos, the otic pit is closely apposed to the r5/6 region of the hindbrain. This apposition cannot be required for otocyst formation, since in both RA-exposed embryos and *kreisler* mutant embryos, the otic pit is separated from the hindbrain neuroepithelium by neural crest-derived mesenchymal cells (Morriss-Kay et al. 1991; Frohman et al. 1993). If there is an otic inductive signal from the hindbrain neuroepithelium to the surface ectoderm, it must either be transmitted laterally within the plane of the two epithelia or be able to traverse the intervening mesenchyme. Our observation of *Fgf-3* expression in otic ectoderm, in continuity with the r4/5/6 hindbrain expression domain and the second pharyngeal arch epithelial domain, argues in favour of simultaneous induction of otic hindbrain and otic placodes in a specific positional relationship to the second arch and pouch. This interpretation is consistent with that of Harrison (1935), who described evidence in amphibian embryos for signals from cardiac mesoderm and chordamesoderm for otic placode specification.

Acknowledgements We thank Dr. C. Dickson for *Fgf-3* probes, Hoffmann-La Roche for all-*trans*-RA, Dr. P. Murphy for initial help with in situ hybridization, Gurman Pall for treatment of mice with RA, Martin Barker for technical assistance, Colin Beesley for photography, and Gail Martin for helpful discussions. This study was funded by grants from Hoffmann-La Roche and the Human Frontier Science Program Organization to GMMK and the Wellcome Trust and MRC to IJM; it was initiated while RM was an MRC scholar.

References

Baird A, Klagsbrun M (1991) Nomenclature meeting: report and recommendations. The fibroblast growth factor family. Ann NY Acad Sci 638: xiii–xvi

Becker N, Seitanidou T, Murphy P, Mattéi M-G, Topilko P, Nieto MA, Wilkinson D, Charnay P, Gilardi-Hebenstreit P (1994) Several receptor tyrosine kinase genes of the *Eph* family are segmentally expressed in the developing hindbrain. Mech Dev 47: 3–17

Couly G, Le Douarin NM (1990) Head morphogenesis in avian chimeras: evidence for a segmental pattern in the ectoderm corresponding to the neuromeres. Development 108: 543–558

Crossley P, Martin GR (1995) The mouse *Fgf-8* gene encodes a family of polypetides and is expressed in regions that direct outgrowth and patterning in the developing embryo. Development 121: 439–451

Deol MS (1964) The abnormalities of the inner ear in *kreisler* mice. J Embryol Exp Morphol 12: 475–490

Dickson C, Peters G (1987) Potential oncogene product related to growth factors. Nature 326: 833–837

Dickson C, Smith R, Brookes S, Peters G (1984) Tumorigenesis by MMTV: proviral activation of a cellular gene in the common integration region int-2. Cell 37: 529–536

Frohman MA, Martin GR, Cordes SP, Halamek L, Barsh GS (1993) Altered rhombomere specific expression and hyoid bone differentiation in the mouse segmentation mutant *kreisler* (*kr*). Development 117: 925–936

Grinberg D, Thurlow J, Watson R, Smith R, Peters G, Dickson C (1991) Transcriptional regulation of the int-2 gene in embryonal carcinoma cells. Cell Growth Differ 2: 137–143

Harrison RG (1935) Factors concerned in the development of the ear in *Amblystoma punctatum*. Anat Rec 64 [Suppl 1]: 38–39

Hunt P, Wilkinson D, Krumlauf R (1991) Patterning the vertebrate head: murine Hox 2 genes mark distinct subpopulations of premigratory and migrating neural crest. Development 112: 43–50

Kaufman MH (1992) The atlas of mouse development. Academic Press, London

Lammer EJ, Armstrong DL (1992) Malformations of hindbrain structures among humans exposed to isotretinoin (13-*cis*-retinoic acid) during early embryogenesis. In: Morriss-Kay GM (ed) Retinoids in normal development and teratogenesis. Oxford University Press, Oxford, pp 281–295

Mahmood R, Kiefer P, Guthrie S, Dickson C, Mason I (1995a) Multiple roles for FGF-3 during cranial neural development in the chicken. Development 121: 1399–1410

Mahmood R, Bresnick J, Hornbruch A, Mahony C, Morton N, Colquhoun K, Martin P, Lumsden A, Dickson C, Mason I (1995b) FGF8 in the mouse embryo: a role in the initiation and maintenance of limb bud outgrowth. Curr Biol 5:797–806

Mansour SL, Martin GR (1988) Four classes of mRNA are expressed from the mouse int-2 gene, a member of the FGF gene family. EMBO J 7: 2035–2041

Mansour SL, Goddard JM, Capecchi MR (1993) Mice homozygous for a targeted disruption of the proto-oncogene int-2 have developmental defects in the tail and inner ear. Development 117: 13–28

Mason I, Fuller-Pace F, Smith R, Dickson C (1994) FGF 7 expression during mouse development suggests roles in myogenesis, forebrain regionalization and epithelial- mesenchymal interactions. Mech Dev 45: 15–30

McKay IJ, Muchamore I, Krumlauf R, Maden M, Lumsden A, Lewis J (1994) The *kreisler* mouse: a hindbrain segmentation mutant that lacks two rhombomeres. Development 120: 2199–2211

Moore R, Casey G, Brookes S, Dixon M, Peters G, Dickson C (1986) Sequence, topography and protein coding potential of mouse int-2. EMBO J 5: 919–924

Morriss GM (1972) Morphogenesis of the malformations induced in rat embryos by maternal hypervitaminosis. J Anat 113: 241–250

Morriss GM, Thorogood PV (1978) An approach to cranial neural crest cell migration in mamalian embryos. In: Johnson MH (ed) Development in mammals, vol 3. Elsevier/North Holland, Amsterdam, pp 363–412

Morriss-Kay GM, Murphy P, Davidson DR, Hill RE (1991) Effects of RA excess on expression of *Hox 2.9* and *Krox 20* and on morphological segmentation in the hindbrain of mouse embryos. EMBO J 10: 2985–2995

Murakami A, Grinberg D, Thurlow J, Dickson C (1993) Identification of positive and negative regulatory elements involved in the retinoic acid/cAMP induction of Fgf-3 transcription in F9 cells. Nucleic Acids Res 21: 5351–5359

Nieto MA, Gilardi-Hebenstreit P, Charnay P, Wilkinson D (1992) A receptor protein tyrosine kinase implicated in the segmental patterning of the hindbrain and mesoderm. Development 116: 1137–1150

Niswander L, Martin GR (1992) Fgf-4 expression during gastrulation, myogenesis, limb and tooth development. Development 114: 755–768

O'Rahilly R (1963) The early development of the otic vesicle in staged human embryos. J Embryol Exp Morphol 11: 741–755

Represa J, León Y, Miner C, Giraldez F (1991) The int-2 proto-oncogene is responsible for induction of the inner ear. Nature 353: 561–563

Ruberte E, Dollé P, Chambon P, Morriss-Kay G (1991) Retinoic acid receptors and cellular retinoid binding protein. II. Their differential pattern of transcription during early morphogenesis in mouse embryos. Development 111: 45–60

Smith R, Petrers G, Dickson C (1988) Multiple RNAs expressed from the int-2 gene mouse embryonal carcinoma cell lines encode a protein with homology to FGFs. EMBO J 7: 1013–1022

Tannahill D, Issacs HV, Close MJ, Peters G, Slack JMW (1992) Developmental expression of *Xenopus* int-2 (FGF-3) gene: activation of mesodermal and neural activation. Development 115: 695–702

Van de Water TR, Ruben RJ (1976) Organogenesis of the ear. In: Hinchliffe R, Harrison D (eds) Scientific foundations of otolaryngology. Heineman, London, pp 173–184

Wilkinson DG (1992) In: Wilkinson DG (ed) In situ hybridization; a practical approach. IRL Press, Oxford

Wilkinson DG, Bailes JA, Champion J, McMahon AP (1987a) A molecular analysis of mouse development from 8 to 10 days p.c. detects changes only in embryonic globin expression. Development 99: 493–500

Wilkinson DG, Bailes JA, McMahon AP (1987b) Expression of the proto-oncogene int-1 is restricted to specific neural cells in developing mouse embryos. Cell 50: 79–88

Wilkinson DG, Peters G, Dickson C, McMahon AP (1988) Expression of the FGF-related proto-oncogene int-2 during gastrulation and neurulation in the mouse. EMBO J 7: 691–695

Wilkinson DG, Bhatt S, McMahon AP (1989) Expression pattern of the FGF-related proto-oncogene int-2 suggests multiple roles in fetal development. Development 105: 131–136

Wood H, Pall G, Morriss-Kay GM (1994) Exposure to RA before or after the onset of somitogenesis reveals separate effects on rhombomeric segmentation and 3 hox B gene expression domains. Development 120: 2279–2285